

Co-evolution of cosmic ray energy spectra, composition, and anisotropies

Bing-Qiang Qiao,^{1,2} Qiang Yuan,^{3,4,*} and Yi-Qing Guo^{5,6,7,†}

¹*Deutsches Elektronen Synchrotron DESY, Platanenallee 6, D-15738, Zeuthen, Germany*

²*Institut für Physik und Astronomie, Universität Potsdam, D-14476, Potsdam, Germany*

³*Division of Dark Matter and Space Astronomy, Purple Mountain Observatory,
Chinese Academy of Sciences, Nanjing 210023, China*

⁴*School of Astronomy and Space Science, University of Science and Technology of China, Hefei 230026, China*

⁵*State Key Laboratory of Particle Astrophysics, Institute of High Energy Physics, Chinese Academy of Sciences, Beijing 100049, China*

⁶*University of Chinese Academy of Sciences, Beijing 100049, China*

⁷*Tianfu Cosmic Ray Research Center, Chengdu, Sichuan 610213, China*

The origin of cosmic rays remains an unresolved fundamental problem in astrophysics. The synergy of multiple observational probes, including the energy spectra, the mass composition, and anisotropy is a viable way to jointly uncover this mystery. In this work, we propose that the energy-dependent of those observables in a wide energy range, from $O(10)$ GeV to ultrahigh energies of 10^{11} GeV, share quite a few correlated features, indicating a strong co-evolution which could be a consequence of the underlying origin of different source populations. We decipher these structures with a four-component model, i.e., the ensemble of Galactic sources, a local source close to the solar system, and the ensemble of two extra-galactic source populations. In this scenario, the $O(10^2)$ GV hardening and $O(10)$ TV bump is due to the contribution of the local source, the knee is due to the maximum acceleration energy of protons by the Galactic source population, the second knee is due to the maximum acceleration energy of iron nuclei by Galactic sources, the dip feature between the two knees is due to the appearance of the extra-galactic component, the ankle comes from the transition from one extra-galactic component to the other, and the spectral suppression at the highest energies arises from the acceleration limit of the second extra-galactic component. The transition from Galactic to extra-galactic origin of cosmic rays occurs around $O(10^8)$ GeV, which is smaller than the ankle energy.

I. INTRODUCTION

After more than one century of the discovery of cosmic rays (CRs), their origin is still unclear. The main challenge is the deflections of charged particles when they propagate in random magnetic fields everywhere in the Universe. It turns out that the arrival directions of CRs are almost isotropic, with small anisotropies (the amplitude is about $10^{-4} \sim 10^{-3}$ below PeV [1]), which erases the original locations of the sources. The other challenge is that the mass composition is not clear for indirect measurements by ground-based experiments. Limited information with relatively large uncertainty makes it difficult to fully address the problems about the origin, acceleration, propagation, and interaction of CRs. In recent years, with the developments of new generation space-borne and ground-based experiments, significant progresses towards precise measurements of CRs have been achieved, which provides a very good opportunity to uncover the mystery of CR physics. Particularly, a synergistic analysis of multi-messenger data, including spectra, anisotropies and mass composition, becomes feasible in light of the improved precision.

The joint discussion of multiple observables of CRs has been done in some works [2–4]. Gaisser et al. [2] proposed a parametric framework using three or four distinct astrophysical components to simultaneously describe the all-particle energy spectrum and mean logarithmic mass ($\langle \ln A \rangle$) of CRs. Extending this methodology and based on LHAASO’s un-

precedented precision in measuring both the energy spectrum ($0.3 - 30$ PeV) and $\langle \ln A \rangle$, Lv et al. [3] and Yao et al. [4] performed a comprehensive analysis spanning nine decades in energy from GeV to 10^{10} GeV. Their systematic investigation reveals compelling evidence for a non-negligible contribution from extragalactic CRs emerging at energies as low as ~ 10 PeV, significantly below the traditional ankle feature (~ 5 EeV) typically associated with the onset of extragalactic dominance. Anisotropies have not been extensively discussed in these works. The co-evolution of the spectra and anisotropies below 1 PeV has been highlighted in Refs. [5–8]. A nearby source at particular direction, with possible alignment effect along with the local regular magnetic field, has been introduced to explain the spectral hardenings at hundreds of GeV and softenings at tens of TeV, as well as the phase reversal of the dipole anisotropies around 100 TeV. However, these studies did not cover the energy range above the knee region.

Therefore, the all particle or individual spectra, composition, and anisotropy of CRs have their respective regions of precise measurement in observations due to the sensitivity of experimental instruments. When used independently to investigate the origin of CRs, regions where experimental observations are not sensitive may fail to provide definitive results. However, by combining these messengers and complementing each other through common evolution, useful information can be obtained. Thus, this work aims to study the origin of CRs through the joint evolution of the total spectrum, component energy spectrum, composition, and anisotropy of CRs. The paper is organized as follows. Sec. II describes the observation data briefly. Sec. III presents our proposed four-component model, with the results given in Sec. IV. Lastly we

* yuanq@pmo.ac.cn

† guoyq@ihep.ac.cn

conclude in Sec. V.

II. OBSERVATIONAL DATA

The measurements of energy spectra for different species have big progresses recently, revealing several new structures of the spectral shapes. A common hardening feature at a rigidity of several hundred GV has been established by many direct detection experiments [9–18]. At slightly higher rigidity, ~ 15 TV, spectral softenings were further revealed by several experiments [14, 15, 17–22]. Above 100 TeV (TV), hints of an additional spectral hardening were shown by a few experiments [23, 24]. This hardening is actually required to be reconciled with the all-particle spectra around PeV energies [25]. For energies above ~ 100 TeV, the measurements are mostly from groundbased indirect detection experiments. Several features have been observed, including the “knee” around $3 \sim 4$ PeV, the “second knee” around 200 PeV, the “ankle” around 5 EeV, and the “GZK cutoff” around 50 EeV [26–36]. There is an additional hardening structure between the two knees, as reported by a few experiments [33, 37, 38]. Given more and more precise measurements, the overall spectra of CRs seem to be very complicated rather than structureless power-laws (see the top panel of Fig. 2). We can note that there are similarities among the spectral features at different energy bands. If we category a hardening and the subsequent softening as one group, we can observe four such groups in the spectra from tens of GeV to the highest end: group 1 from 10 GeV to 100 TeV, group 2 from 10 TeV to 10 PeV, group 3 from 10 PeV to 1 EeV, and group 4 from 1 EeV to 100 EeV. Those similarities indicate that there are possible common mechanisms to form (at least some of) such structures.

The spectra of individual species are crucial to the understanding of the CR physics. For energies below ~ 100 TeV, direct detection experiments can well measure the individual spectra, which reveal the group A structures for several major species. At higher energies, however, it is usually difficult to distinguish different compositions with indirect detection technique, and the individual spectra have large (systematic) uncertainties. The measurements of average logarithmic mass number of particles, $\langle \ln A \rangle$, can in turn reflect the relative fractions of different species. Such measurements can be done via measuring the lateral distribution of Cherenkov light [39], the muon content in showers [31, 40, 41], or the longitudinal developments of showers [42–44]. See Ref. [45] for an attempt to infer the average logarithmic mass from those observables. The results of $\langle \ln A \rangle$ in a wide energy range are shown in the second panel of Fig. 2. For energies below PeV, we directly calculate $\langle \ln A \rangle$ based on the individual spectra of the main species measured by ATIC [9], CREAM [10], and AMS-02 [46]. With the increase of energy, the value of $\langle \ln A \rangle$ shows an increase from ~ 1.0 at 10 GeV to a plateau of ~ 1.5 at TeV-PeV, and increases again after PeV to reach a peak value of $3.0 \sim 4.0$ around 100 PeV. Then it decreases to a valley of about 0.5 at about 1 EeV, after which it increases again.

Anisotropies of arrival directions of CRs have been measured by groundbased air shower or underground muon de-

tectors. It is obviously that for the energies less than \sim PeV, the amplitude of anisotropy does not exhibit a simple power-law increasing with energy. Instead, it reaches a maximum around 10 TeV and then decreases to a minimum near 100 TeV, forming a distinct “trough”-like structure. Remarkably, the anisotropy phase simultaneously undergoes a reversal, from alignment with the IBEX-inferred local magnetic field direction to that of the Galactic center, resulting in a complementary “reversal” pattern [1, 47]. These fine-scale features are believed to be closely related to the influence of nearby sources, as suggested by recent theoretical studies [6, 7, 48]. Of particular significance, the Pierre Auger Observatory has performed a detailed analysis of the first-harmonic modulation in the right ascension (R.A.) distribution of CRs with energy more than several tens of PeV, determining both the dipole amplitude and phase in equatorial coordinates. For energies above 8 EeV, the measured dipole amplitude reaches $0.060^{+0.010}_{-0.009}$, with a statistical significance of 6σ , and the corresponding phase is observed at $98^\circ \pm 9^\circ$ [49]. Furthermore, at lower energies (< 8 EeV), the dipole amplitude evolves gradually, decreasing from approximately 1% at 30 PeV to about 0.1% around 1 EeV, then rising to nearly 10% at 30 EeV. Meanwhile, the dipole phase shows a smooth transition: initially aligned with the Galactic center direction, it gradually shifts toward $\alpha \sim 100^\circ$, with the transition occurring at a few EeV [50]. This behavior strongly suggests an extragalactic origin for these CRs.

It is very interesting to note that, the structures of the spectra, composition, and anisotropies show correlated evolution with energy. When there is spectral change (hardening or softening) on the energy spectra, some imprints on the $\langle \ln A \rangle$ and large-scale anisotropies (amplitude and phase) can be seen. For example, the softenings at ~ 15 TV and ~ 3 PeV in the spectrum correspond to local minima of $\langle \ln A \rangle$, while the hardenings around 100 TeV and 30 PeV correspond to local maxima of $\langle \ln A \rangle$. Moreover, the amplitude and phase of the large-scale anisotropies also show analogous variations at corresponding characteristic energies. Such a co-evolution of spectra, composition, and anisotropies give strong support of a picture that CRs at different energy ranges have different origin. The sum of these source populations, with different acceleration limits, source composition, and spatial distributions, give rise to complicated but correlated structures of their spectra, $\langle \ln A \rangle$, and anisotropies.

III. A FOUR-COMPONENT MODEL

In this work, we propose to understand the observed energy spectrum, composition and anisotropy of CRs with energies from $O(10)$ GeV to about 10^{20} eV using a four-component model, which includes the Galactic background sources (component A), one Galactic nearby source (component B), and two extragalactic source populations (components C and D). Note that two extragalactic source components are required here to fit the data of spectra and composition [2–4]. Fig. 1 is a cartoon plot to show different source components mentioned above, illustrating their contribution to the energy spectra and

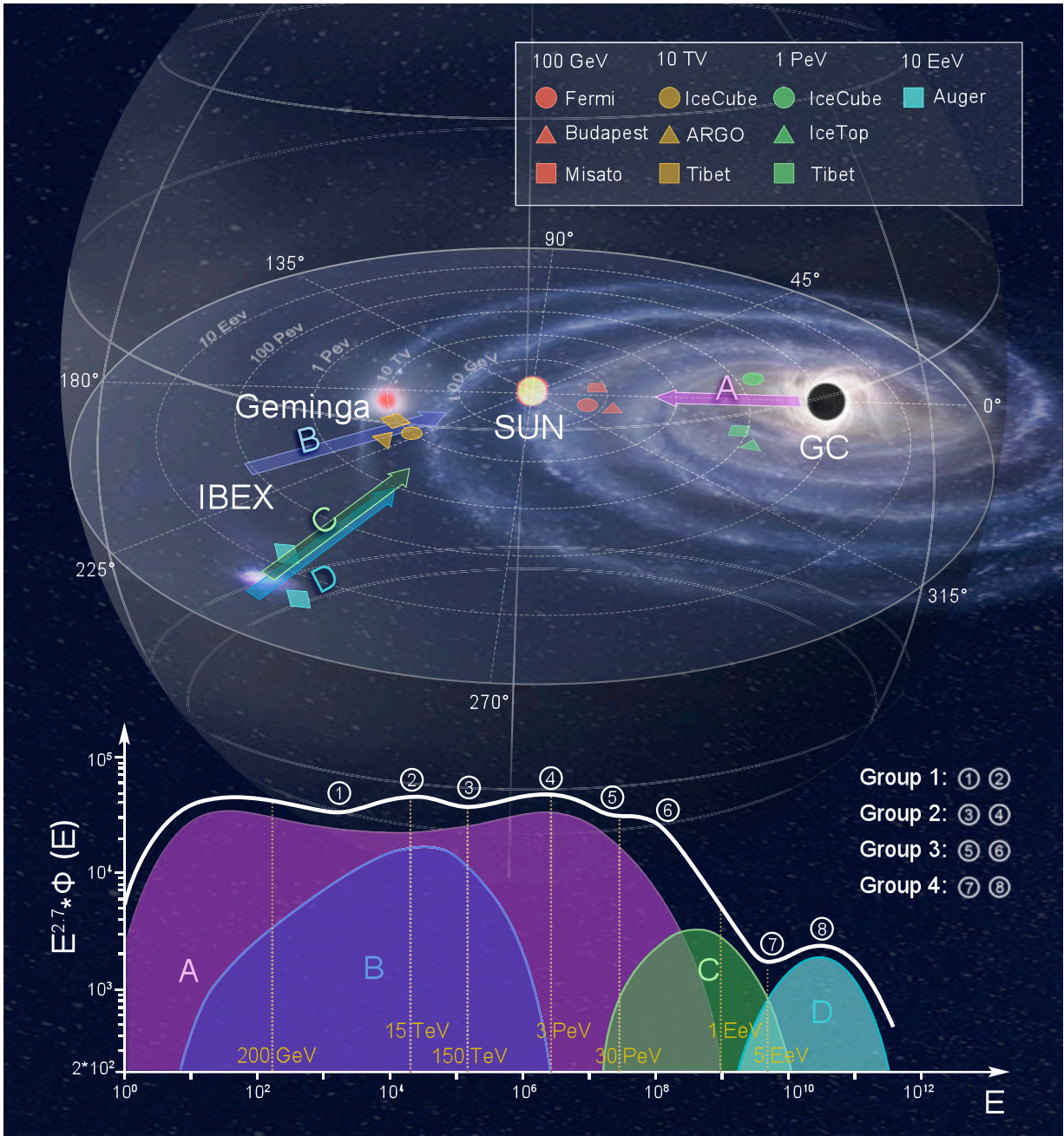


FIG. 1. Illustration of the contributions to CR spectra and arrival directions from different source components. Filled circles, triangles, and squares show the measured directions of anisotropies at different typical energies (red for 100 GeV, brown for 10 TeV, green for 1 PeV, and cyan for 10 EeV). It shows the evolution of the anisotropy direction from the Galactic center (GC) at ~ 100 GeV, to approximately the anti-GC (perhaps aligned with the local magnetic field as labelled by IBEX) around 10 TeV, to the GC again around PeV, and finally to the direction shown by green and cyan arrows around 10 EeV. The bottom part shows how the sum of these components result in complicated “ankle-knee” structures in the spectra.

arrival directions (shown by arrows). The algebraic sum of these source components is responsible to the structures in the all-particle spectra and the average logarithmic mass number, and the vector sum of these components gives energy evolution of the anisotropy amplitude and phase.

A. Galactic background sources

Various types of sources in the Galaxy have been found to be able to accelerate CRs, such as supernova remnants, massive star clusters, accretion disks and jets of black holes and so on. While the detailed acceleration characteristics of these sources may be uncertain, phenomenologically a continuous

source distribution with an average accelerated spectrum is usually assumed, and the produced particles are injected in the Galaxy, experiencing a diffusive transport process. The transport equation can be written as [51]

$$\begin{aligned} \frac{\partial \psi_A(\vec{r}, p, t)}{\partial t} = & q_A(\vec{r}, p, t) + \nabla \cdot (D_{xx} \nabla \psi - \vec{V}_c \psi) \\ & + \frac{\partial}{\partial p} \left[p^2 D_{pp} \frac{\partial}{\partial p} \frac{1}{p^2} \psi \right] - \frac{\partial}{\partial p} \left[\dot{p} \psi - \frac{p}{3} (\nabla \cdot \vec{V}_c) \psi \right] \\ & - \frac{\psi}{\tau_f} - \frac{\psi}{\tau_r}, \end{aligned} \quad (1)$$

where ψ_A is the CR density per particle momentum interval at position \vec{r} , $q_A(\vec{r}, p, t)$ is the source function, $D_{xx}(\vec{r}, p)$ is the diffusion coefficient, \vec{V}_c is the convection velocity, $D_{pp}(\vec{r}, p)$ is the diffusion coefficient in the momentum space which describes the reacceleration of particles during the propagation, \dot{p} is the momentum loss rate, τ_f and τ_r are the fragmentation and radioactive decaying time scales. The convection and reacceleration are important for low energy CRs. For the energy range relevant for this work ($E \gtrsim 30$ GeV), their effects can be neglected. Usually a cylinder is adopted to describe the geometry of the propagation halo. Free escape is assumed at the border of the halo, namely $\psi_A(r, z, p) = \psi_A(r_h, z, p) = \psi_A(r, \pm z_h, p) = 0$.

The spatial distribution of the sources is parameterized as $f(r, z) = (r/r_\odot)^{1.25} \exp[-3.56(r - r_\odot)/r_\odot - |z|/(0.2 \text{ kpc})]$ [52], where $r_\odot = 8.5$ kpc. The injection spectrum of CR nuclei are assumed to be an exponentially cutoff power-law function of particle rigidity \mathcal{R} as $q_A(\mathcal{R}) = q_0^A \mathcal{R}^{-\nu_A} \exp[-\mathcal{R}/\mathcal{R}_c^A]$, where q_0^A is the normalization factor, ν_A is the spectral index, and \mathcal{R}_c^A is the cutoff rigidity. Note that one or more breaks of the injection spectrum at low energies may be necessary to fit the wide-band data [53, 54]. For the purpose of this work, we find that one single power-law with an exponentially cutoff is enough.

In the conventional model, the spatial diffusion coefficient is typically assumed to be uniform everywhere throughout the Galaxy. However, it is natural to expect that the diffusion coefficient should be spatially dependent, due to the non-uniform properties of the interstellar medium (ISM). This picture is supported by recent observations of very-high-energy γ -ray halos surrounding middle-aged pulsars [55, 56]. It has been shown that the derived diffusion coefficient around these pulsars is smaller by $10^2 - 10^3$ times than the average diffusion coefficient inferred from the CR secondary-to-primary ratio (e.g., [57]). Consequently, we employ the spatially dependent propagation (SDP) scenario [58, 59] to describe the transport of particles. The diffusion coefficient is smaller in a relatively thin disk (with vertical height $|z| \leq \xi z_h$), and bigger in the halo (with $|z| > \xi z_h$), where z_h is the height of the transport halo. A smooth connection of the diffusion coefficient between the disk and the halo is assumed. The detailed function form of the SDP part of the diffusion coefficient can be found in [60].

At high energies (e.g., $\mathcal{R} > \text{PV}$), the gyro-radius of particles ($\gtrsim \text{pc}$) may be comparable to the coherent length of the local magnetic field, and the CR transport becomes less sensitive to small inhomogeneities of the ISM. In such a case, the dif-

fusion coefficient should be more uniform, and returns to the one in the halo. Therefore, the diffusion coefficient is written as

$$D_{xx}(r, z, \mathcal{R}) = \begin{cases} D_0 F(r, z) \beta^\eta \left(\frac{\mathcal{R}}{\mathcal{R}_0} \right)^{\delta_0 F(r, z)}, & \mathcal{R} < 1 \text{ PV} \\ D_0 \beta^\eta \left(\frac{\mathcal{R}}{\mathcal{R}_0} \right)^{\delta_0}, & \mathcal{R} > 1 \text{ PV} \end{cases}, \quad (2)$$

where β is the particle's velocity in unit of the light speed, D_0 and δ_0 are constants characterizing the diffusion coefficient and its rigidity dependence in the halo, η is a phenomenological constant in order to fit the low-energy data, and $F(r, z)$ describes the spatial variation of the diffusion coefficient [60].

In this work, we adopt the diffusion re-acceleration model, with the diffusive re-acceleration coefficient D_{pp} , which correlates with D_{xx} via $D_{pp} D_{xx} = \frac{4p^2 V_A^2}{3\delta(4-\delta^2)(4-\delta)}$, where V_A is the Alfvén velocity, p is the momentum, and δ is the rigidity dependence slope of D_{xx} [61]. We use the DRAGON code to solve the transport equation [62]. For energies smaller than tens of GeV, the fluxes of CRs are further suppressed by the solar modulation effect, for which we use the force-field approximation [63]. The main propagation parameters are: $D_0 = 8.1 \times 10^{28} \text{ cm}^2 \text{ s}^{-1}$, $\delta_0 = 0.56$, $\eta = 0.05$, $N_m = 0.9$, $\xi = 0.09$, $n = 4$, $V_A = 6.0 \text{ km s}^{-1}$, $z_h = 4.5 \text{ kpc}$. The reference rigidity is $\mathcal{R}_0 \equiv 1 \text{ GV}$. We find that a unified spectral index of $\nu_A = 2.41$ and cutoff rigidity of $\mathcal{R}_c^A = 8 \text{ PV}$ can well fit the spectra of individual species and all particles, and the average logarithmic mass. The normalization parameter of each species can be found in Table I.

B. Galactic nearby source

Local source(s) has been proposed as one possible origin of the observed features of energy spectra (~ 200 GV hardenings and ~ 15 TV softenings) and dipole anisotropies [5–7]. Among the observed candidate sources such as supernova remnants, it has been shown that, under the framework of slow diffusion in the Galactic disk, Geminga could be the right source to have proper contribution to the locally observed CR spectra [64]. The direction of Geminga, (R.A., Decl.) = ($6^h 34^m$, $17^\circ 46'$), is also consistent with the direction of the dipole anisotropy phase below 100 TeV^1 . The electrons and positrons produced by the pulsar wind nebula associated with the local source can further explain the positron excess and the total electron plus positron spectra [65]. Here we also take Geminga as an illustration of local source. Its distance is adopted as 250 pc , and age is adopted as $3.4 \times 10^5 \text{ yr}$ [66].

The propagation of nuclei from the nearby source can be calculated using the Green's function method, assuming a spherical geometry with infinite boundary conditions. Assuming instantaneous injection from a point source, the CR density as a function of space, energy, and time can be calculated

¹ Considering the alignment effect along the local regular magnetic field [47], other sources located in the outer Galaxy hemisphere may also give the right dipole anisotropy [48].

TABLE I. Injection spectral parameters of the four source components.

	Component A			Component B			Component C			Component D		
Element	q_0^A	ν_A	\mathcal{R}_c^A	q_0^B	ν_B	\mathcal{R}_c^B	q_0^{C*}	ν_C	\mathcal{R}_c^C	q_0^{D*}	ν_D	\mathcal{R}_c^D
	$[(\text{m}^2 \cdot \text{sr} \cdot \text{s} \cdot \text{GeV})^{-1}]$		[PV]	$[\text{GeV}^{-1}]$		[TV]	$[(\text{m}^2 \cdot \text{sr} \cdot \text{s} \cdot \text{GeV})^{-1}]$		[EV]	$[(\text{m}^2 \cdot \text{sr} \cdot \text{s} \cdot \text{GeV})^{-1}]$		[EV]
p	2.83×10^{-2}	2.41	8	1.8×10^{52}	2.32	40	5.0×10^1	2.45	1.0	6.8×10^{-5}	1.95	15
He	1.29×10^{-3}	2.41	8	1.5×10^{52}	2.32	40	6.0×10^{-1}	2.45	1.0	2.5×10^{-5}	1.95	15
C	4.47×10^{-5}	2.41	8	4.6×10^{50}	2.32	40	1.0×10^{-1}	2.45	1.0	4.0×10^{-6}	1.95	15
N	7.53×10^{-6}	2.41	8	4.5×10^{49}	2.32	40	3.0×10^{-2}	2.45	1.0	—	—	—
O	5.43×10^{-5}	2.41	8	4.7×10^{50}	2.32	40	6.0×10^{-2}	2.45	1.0	2.0×10^{-6}	1.95	15
Ne	1.14×10^{-5}	2.41	8	8.0×10^{49}	2.32	40	4.0×10^{-2}	2.45	1.0	—	—	—
Mg	1.42×10^{-5}	2.41	8	8.0×10^{49}	2.32	40	2.0×10^{-2}	2.45	1.0	—	—	—
Si	1.09×10^{-5}	2.41	8	7.5×10^{49}	2.32	40	1.0×10^{-2}	2.45	1.0	—	—	—
Fe	1.02×10^{-5}	2.41	8	3.5×10^{49}	2.32	40	1.0×10^{-3}	2.45	1.0	1.0×10^{-7}	1.95	15

[†]The normalization is set at kinetic energy per nucleon $E_k = 100 \text{ GeV/n}$.

^{*}The normalization is set at particle's total kinetic energy $E = 1 \text{ GeV}$.

as

$$\psi_B(r, E, t) = \frac{q_B(E)}{(\sqrt{2\pi}\sigma)^3} \exp\left(-\frac{r^2}{2\sigma^2}\right), \quad (3)$$

where $q_B(E)$ is the injection spectrum as a function of rigidity, $\sigma(E, t) = \sqrt{2D(E)t}$ is the effective diffusion length within time t . The diffusion coefficient $D(E)$ takes the solar system value of Eq. (2). The function form of $q_B(E)$ is assumed to be power-law with an exponential cutoff, i.e., $q_B(E) = q_0^B E^{-\nu_B} \exp(-E/(Z\mathcal{R}_c^B))$. Through fitting to the data, we find that the spectral index ν_B is about 2.32, and the cutoff rigidity is about 40 TV for all species. The normalization parameter q_0^B of different species is given in Table I.

C. Extragalactic low- and high-energy sources

With the increase of energy, it is expected that CRs should experience a transition from the Galactic origin to the extragalactic origin. The acceleration end of Galactic sources and the transition energy is unclear yet. Different models are proposed to explain the ankle and cutoff structures of ultrahigh energy CRs [34, 35], which predict different transition energy. In one type of models, the highest energy suppression of the spectrum is due to the GZK process, i.e., interaction between protons and the cosmic microwave background (CMB) photons [67]. In this scenario the ankle is explained by the pair production of electrons and positrons due to the $p\gamma$ interaction. This model requires that the composition of ultrahigh energy CRs is dominated by protons, which seems to be different from the recent measurements [68]. The other type of models suggest the highest energy cutoff is due to the acceleration limit of extragalactic sources and the ankle is ascribed to the transition from Galactic origin to extragalactic origin [69, 70]. In this case, the appearance of the extragalactic component is higher than several EeV, and there will be a gap between 0.1 and 1 EeV if assuming that the knee is due to the acceleration limit of protons from Galactic sources. A second

Galactic component (Component B) was introduced to fill this gap by Hillas [71].

In this work, we basically follow the latter type of models, but interpret the Galactic component B as an additional extragalactic component. Therefore in our case, we have two extragalactic components, C and D, to reproduce the multimessenger data. The two extragalactic components were also found to be necessary to explain the measured mass composition [2, 3]. The spectral form for the extragalactic components is parameterized as [72]

$$\psi_i(E) = q_0^i E^{-\nu_i} \times \exp\left(-\frac{E}{Z\mathcal{R}_c^i}\right) \times \frac{1}{\cosh\left[\left(\frac{Z\mathcal{R}_s}{E}\right)^\beta\right]}, \quad (4)$$

where i denotes the low-energy (component C) and high-energy (component D), q_0^i is the flux normalization, ν_i is the spectral index, Z is the particle charge, \mathcal{R}_c^i is the cutoff rigidity. The cosh term describes the shielding effect of Galactic magnetic field to extragalactic CRs, with characteristic shielding rigidity $\mathcal{R}_s = 60 \text{ PeV}$, and finally $\beta = 1.6$ is a parameter to describe the smoothness of the low-energy shielding. The relevant parameters of components C and D are summarized in Table I.

IV. RESULTS

The results of the model fittings together with the measurements for the energy spectra, $\langle \ln A \rangle$, amplitudes and phases of the dipole anisotropies are shown in Figs. 2 and 3. Below we discuss each of these observables.

A. Spectra of all-particle and individual composition

Panel (a) of Fig. 2 shows the all-particle energy spectrum expected from the four source components (blue for A, red for B, cyan for C, and green for D) and their sum (black solid

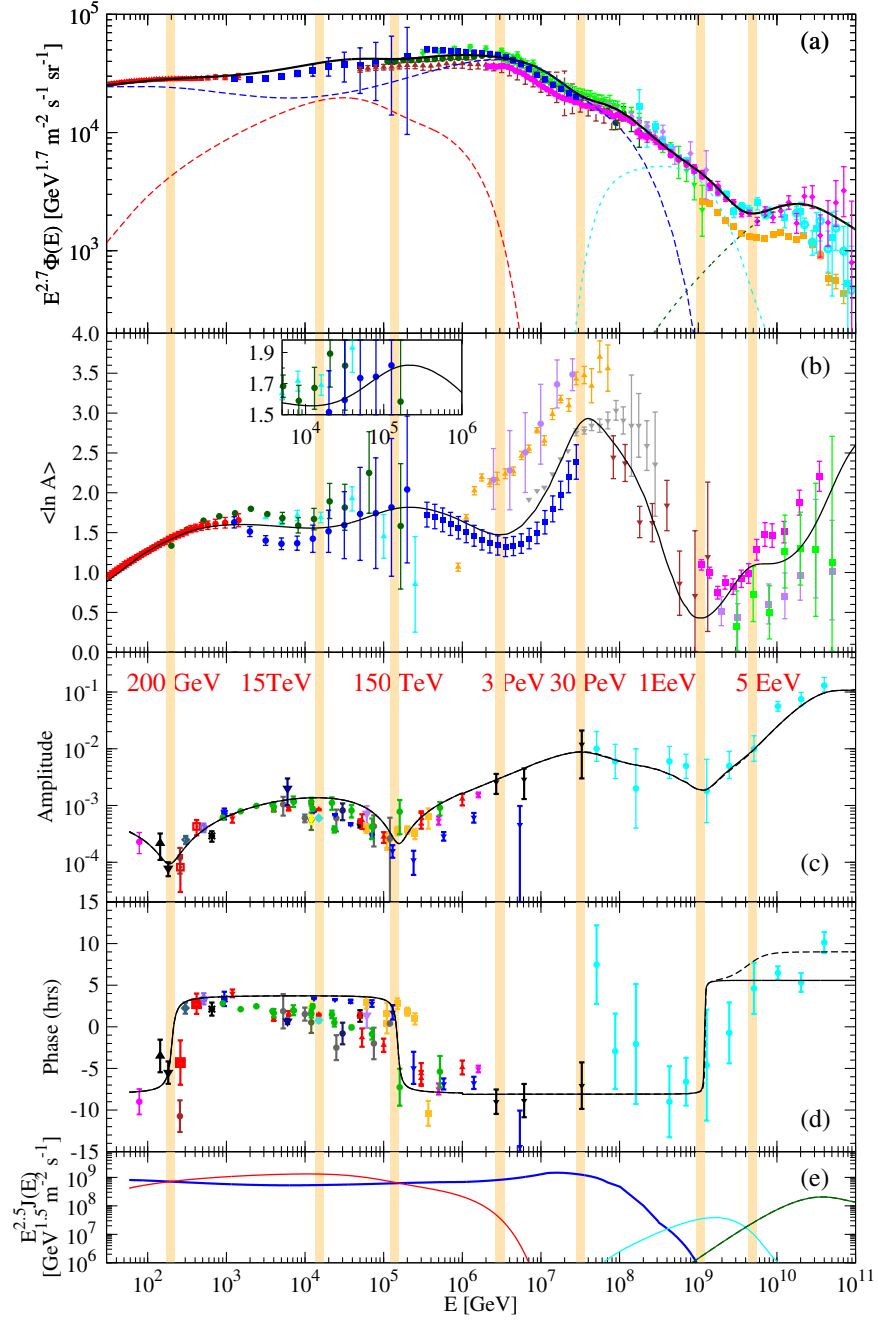


FIG. 2. The co-evolution of the all-particle spectrum (panel a), the mean logarithmic mass $\langle \ln A \rangle$ (panel b), the amplitude (panel c) and phase (panel d) of the dipole component of the large scale anisotropies, and the strength of CR streaming (defined as $J(E) = |D(E)\nabla\phi|$; panel e), for energies from tens of GeV to ~ 100 EeV. Black solid lines show the total model calculation results. In panels a and e, the contributions from components A (blue), B (red), C (cyan), and D (green) are also shown. The dashed line in panel d shows the expected phase for a different direction of the extragalactic component D from that of component C. The vertical bands label the characteristic energies of correlated features of the multi-messenger observables. References of the measurements are: energy spectra [12, 13, 19, 32, 34, 38–41, 73–85]; mean logarithmic mass [31, 39, 41, 45, 80, 86–91]; anisotropies [49, 50, 92–120]. Note that for energies ≤ 100 TeV, the total spectra and mean logarithmic mass are derived from direct detection experiments such as AMS-02, CREAM, and NUCLEON.

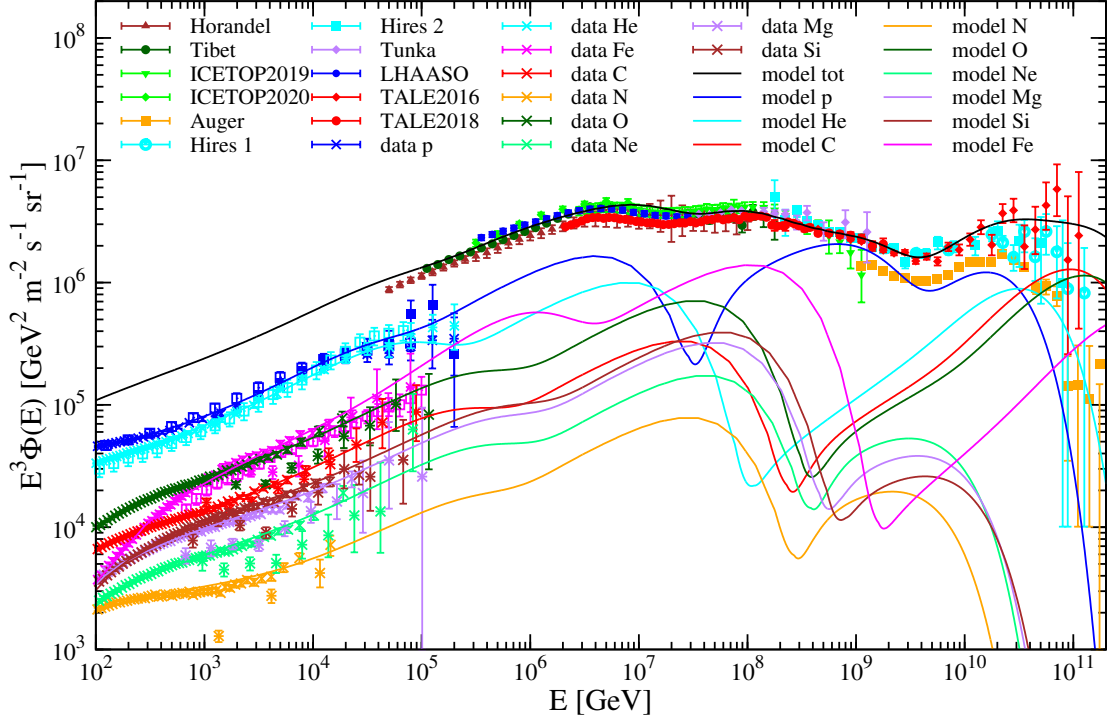


FIG. 3. Model calculated spectra of all particles and several major species (p, He, C, N, O, Ne, Mg, Si, Fe), compared with the measurements. References of the all-particle spectrum are the same as in Fig. 2, and references for individual mass groups are: protons [12, 14, 19, 86], He [13, 15, 19, 77], C [77, 78], N [76, 78], O [77, 78], Ne [75, 78], Mg [75, 78], Si [75, 78], Fe [74, 78, 121].

line). Note that, for the low-energy part below ~ 100 TeV, the spectrum and $\langle \ln A \rangle$ are derived according to the direct measurements of major compositions such as protons, He, CNO, NeMgSi, and Fe. The main features of the spectrum, e.g., the four groups “hardening-softening” structures, can be properly reproduced by the sum of different source components, reflecting complicated origin of CRs over the entire energy range. The group 1 “hardening-softening” feature between 10 GeV and 100 TeV comes mainly from the superposition of Galactic components A and B. Due to the sum of all compositions, the actual hardening energy of the all-particle spectrum is about TeV. With the decrease of contribution from component B above tens of TeV, the recovery of component A dominance results in the group 2 feature, producing the knee with its acceleration limit. The appearance of the extragalactic component C results in a hardening around 30 PeV, and the acceleration limit of iron from component A results in the second knee around 200 PeV. These two effects form the group 3 feature. Finally, the transition between extragalactic component C and D gives rise to the ankle around 5 EeV, and the acceleration limit of component D gives the highest energy cutoff (group 4).

B. Mean logarithmic mass

The mean logarithmic mass is another critical messenger carrying information about the composition of CRs. It is very interesting to see that, the spectral structures due to different source components also leave corresponding imprints on the mean logarithmic mass, primarily due to the basic assumption of this work, that the spectra of different compositions have a charge-dependence. Therefore, whenever a new source component starts to appear, the mean mass composition varies from heavy to light since the new component is always proton dominated at first. When the contribution from the new component starts to decrease, the composition becomes heavy again. Then we see that each group of hardening-softening spectral feature corresponds to a “bump-dip” structure of $\langle \ln A \rangle$, as labelled by vertical bands in Fig. 2. Such a correlation has been highlighted by the recent high-precision measurements of the all-particle spectrum and $\langle \ln A \rangle$ with LHAASO [41]. Although relatively large uncertainties of the measurements of $\langle \ln A \rangle$ exist in other energy bands, the correlation between $\langle \ln A \rangle$ and the spectra is visible.

C. Large scale anisotropy

The dipole component of the large scale anisotropy reflects the streaming of CRs. The measured amplitudes and phases of the dipole anisotropy show complicated energy evolution, which may reflect the sum effect of multiple streamings. As shown in panels (c) and (d) of Fig. 2, the characteristic energies of the anisotropy features also show good correspondence with those of spectra and $\langle \ln A \rangle$. The dipole anisotropy can be well understood in the four component source model.

For source component A, the CR streaming points from the GC to anti-GC. The nearby source (component B) generates a different streaming with direction pointing from the source to the Earth. The sum of the two streamings then gives the observed anisotropy evolution. At ~ 150 TeV a phase reversal is expected due to the nearby source streaming becomes subdominant compared with the Galactic background sources. It is interesting to note that at ~ 100 GeV another phase reversal is expected due to the same reason as the 150 TeV reversal. The new observations of proton anisotropy by Fermi space telescope seems to show such a trend [119]. However, the significance is relatively low due to limited statistics. Future measurements by space-borne detector such as HERD [122] and VLAST [123] are able to test this expected anisotropy feature. The local regular magnetic field may further regulate the directions of low-energy CR streamings, resulting in changes of detailed numbers of the phase [47, 48]. The basic picture discussed in this work still holds, and we do not focus on such details.

From ~ 150 TeV up to the end of the Galactic contribution, the main contribution to the anisotropy is component A, with phase of the GC. From ~ 30 PeV, component C starts to take effect, and we can see a break of the energy-dependence of the amplitude. The phase keeps unchanged until ~ 1 EeV, at which the streaming from source component C becomes dominant. Note that, due to the limited knowledge about the propagation of CRs in the extragalactic space, we adopt a phenomenological approach to calculate the anisotropy of extragalactic sources via simply introducing a streaming with given direction, and adjusting its strength and energy-dependent slope to fit the measurements. Around 5 EeV, component D further dominates over component C, and additional changes may exist if the phases of components C and D are different, as illustrated by the dashed line in panel (d) of Fig. 2.

V. CONCLUSION AND DISCUSSION

Through a detailed investigation of the multi-messenger observables of CRs, we notice that in the very wide energy range from tens of GeV to highest end of the CR spectra, the energy spectrum, average logarithmic mass, and large-scale anisotropy co-evolve with energy. Such a co-evolution indi-

cates that these features share common origins. We then propose a four-component model, with two Galactic source components and two extragalactic source components, to account for the wide-band observational features. For each component, we assume different compositions share similar rigidity spectrum and adjust their abundance to fit the measurements. The observed features of the spectrum, $\langle \ln A \rangle$, and dipole anisotropy amplitude and phase, can be reproduced as the relative weights of different components vary with energy. Particularly, the spectrum is the algebraic sum of the four components, and the anisotropy is the vector sum of the four components.

The structures of the energy spectrum can be classified into 4 groups of “hardening-softening” features. From low to high energy, they are group 1 with $O(10^2)$ GV hardening and $O(10)$ TV softening, group 2 with $O(10^2)$ TeV hardening and ~ 3 PeV softening (also known as the “knee”), group 3 with ~ 30 PeV hardening and ~ 200 PeV softening (the second “knee”), and group 4 with ~ 5 EeV hardening (the “ankle”) and the ~ 50 EeV softening (the “GZK cutoff”). Correspondingly there are imprints on $\langle \ln A \rangle$ and dipole anisotropy amplitude and phase at these characteristic energies. The group 1 feature is interpreted as the sum of Galactic source components A and B. The CR streaming from component B dominates over component A between ~ 100 GeV and 10 TeV, resulting in two phase reversals of the dipole anisotropy. With the decrease of the contribution from component B for energy above tens of TeV, the recovery of component A and its acceleration limit give the group 2 feature. The appearance of extragalactic component C and the decrease of component A gives the group 3 feature, and finally the transition from component C to component D and the acceleration limit of component D produce the group 4 feature.

While such a four component scenario can account for the complicated structures on the energy spectrum, $\langle \ln A \rangle$, and dipole anisotropy, we note that the current measurements have relatively large uncertainties, especially for the composition and anisotropy measurements above tens of PeV. Measurements of the mass composition between TeV and 100 TeV, as well as the anisotropy below TeV, relevant to direct detection experiments, are also uncertain. Improved measurements of these quantities in both low and high energy bands by future direct and indirect detection experiments are very crucial in further constraining the source populations of CRs.

ACKNOWLEDGMENTS

This work is supported in China by National Key R&D program of China under the grant 2024YFA1611402 and the National Natural Science Foundation of China (No. 12220101003, 12333006, 12275279) and the Project for Young Scientists in Basic Research of Chinese Academy of Sciences (No. YSBR-061).

[1] M. Ahlers and P. Mertsch, Progress in Particle and Nuclear Physics **94**, 184 (2017), 1612.01873.

[2] T. K. Gaisser, T. Stanev, and S. Tilav, Frontiers of Physics **8**, 748 (2013), 1303.3565.

- [3] X.-J. Lv, X.-J. Bi, K. Fang, Y.-Q. Guo, H.-H. He, L.-L. Ma, P.-F. Yin, Q. Yuan, and M.-J. Zhao, *Astrophys. J.* **979**, 225 (2025), 2403.11832.
- [4] Y.-H. Yao, Y.-Q. Guo, and W. Liu, *arXiv e-prints arXiv:2403.13482* (2024), 2403.13482.
- [5] L. G. Sveshnikova, O. N. Strelnikova, and V. S. Ptuskin, *Astroparticle Physics* **50**, 33 (2013), 1301.2028.
- [6] W. Liu, Y.-Q. Guo, and Q. Yuan, *J. Cosmol. Astropart. Phys.* **2019**, 010 (2019), 1812.09673.
- [7] B.-Q. Qiao, W. Liu, Y.-Q. Guo, and Q. Yuan, *J. Cosmol. Astropart. Phys.* **2019**, 007 (2019), 1905.12505.
- [8] B.-Q. Qiao, Q. Luo, Q. Yuan, and Y.-Q. Guo, *Astrophys. J.* **942**, 13 (2023), 2201.06234.
- [9] A. D. Panov, J. H. Adams, Jr., H. S. Ahn, K. E. Batkov, G. L. Bashindzhagyan, J. W. Watts, J. P. Wefel, J. Wu, O. Ganel, T. G. Guzik, et al., *Bull. Russ. Acad. Sci. Phys.* **71**, 494 (2007), astro-ph/0612377.
- [10] H. S. Ahn, P. Allison, M. G. Bagliesi, J. J. Beatty, G. Bigongiari, J. T. Childers, N. B. Conklin, S. Coutu, M. A. DuVernois, O. Ganel, et al., *Astrophys. J. Lett.* **714**, L89 (2010), 1004.1123.
- [11] O. Adriani, G. C. Barbarino, G. A. Bazilevskaya, R. Bellotti, M. Boezio, E. A. Bogomolov, L. Bonechi, M. Bongi, V. Bonvicini, S. Borisov, et al., *Science* **332**, 69 (2011), 1103.4055.
- [12] M. Aguilar, D. Aisa, B. Alpat, A. Alvino, G. Ambrosi, K. Andeen, L. Arruda, N. Attig, P. Azzarello, A. Bachlechner, et al., *Phys. Rev. Lett.* **114**, 171103 (2015).
- [13] M. Aguilar, D. Aisa, B. Alpat, A. Alvino, G. Ambrosi, K. Andeen, L. Arruda, N. Attig, P. Azzarello, A. Bachlechner, et al., *Phys. Rev. Lett.* **115**, 211101 (2015).
- [14] Q. An, R. Asfandiyarov, P. Azzarello, P. Bernardini, X. J. Bi, M. S. Cai, J. Chang, D. Y. Chen, H. F. Chen, J. L. Chen, et al., *Science Advances* **5**, eaax3793 (2019), 1909.12860.
- [15] F. Alemanno, Q. An, P. Azzarello, F. C. T. Barbato, P. Bernardini, X. J. Bi, M. S. Cai, E. Catanzani, J. Chang, D. Y. Chen, et al., *Phys. Rev. Lett.* **126**, 201102 (2021), 2105.09073.
- [16] O. Adriani, Y. Akaike, K. Asano, Y. Asaoka, M. G. Bagliesi, E. Berti, G. Bigongiari, W. R. Binns, M. Bongi, P. Brogi, et al., *Phys. Rev. Lett.* **125**, 251102 (2020), 2012.10319.
- [17] O. Adriani, Y. Akaike, K. Asano, Y. Asaoka, E. Berti, G. Bigongiari, W. R. Binns, M. Bongi, P. Brogi, A. Bruno, et al., *Phys. Rev. Lett.* **129**, 101102 (2022), 2209.01302.
- [18] O. Adriani, Y. Akaike, K. Asano, Y. Asaoka, E. Berti, G. Bigongiari, W. R. Binns, M. Bongi, P. Brogi, A. Bruno, et al., *Phys. Rev. Lett.* **130**, 171002 (2023), 2304.14699.
- [19] Y. S. Yoon, T. Anderson, A. Barrau, N. B. Conklin, S. Coutu, L. Derome, J. H. Han, J. A. Jeon, K. C. Kim, M. H. Kim, et al., *Astrophys. J.* **839**, 5 (2017), 1704.02512.
- [20] E. Atkin, V. Bulatov, V. Dorokhov, N. Gorbunov, S. Filipov, V. Grebenyuk, D. Karmanov, I. Kovalev, I. Kudryashov, A. Kurganov, et al., *Soviet Journal of Experimental and Theoretical Physics Letters* **108**, 5 (2018), 1805.07119.
- [21] G. H. Choi, E. S. Seo, S. Aggarwal, Y. Amare, D. Angelaszek, D. P. Bowman, Y. C. Chen, M. Copley, L. Derome, L. Eraud, et al., *Astrophys. J.* **940**, 107 (2022).
- [22] A. Albert, R. Alfaro, C. Alvarez, J. R. Angeles Camacho, J. C. Arteaga-Velázquez, K. P. Arunbabu, D. Avila Rojas, H. A. Ayala Solares, E. Belmont-Moreno, C. Brisbois, et al., *Phys. Rev. D* **105**, 063021 (2022), 2204.06662.
- [23] F. Alemanno, C. Altomare, Q. An, P. Azzarello, F. C. T. Barbato, P. Bernardini, X. J. Bi, I. Cagnoli, M. S. Cai, E. Casilli, et al., *Phys. Rev. D* **109**, L121101 (2024), 2304.00137.
- [24] F. Varsi, S. Ahmad, M. Chakraborty, A. Chandra, S. R. Dugad, U. D. Goswami, S. K. Gupta, B. Hariharan, Y. Hayashi, P. Jagadeesan, et al., *Phys. Rev. Lett.* **132**, 051002 (2024).
- [25] C. Yue, P.-X. Ma, Q. Yuan, Y.-Z. Fan, Z.-F. Chen, M.-Y. Cui, H.-T. Dai, T.-K. Dong, X. Huang, W. Jiang, et al., *Frontiers of Physics* **15**, 24601 (2020), 1909.12857.
- [26] T. V. Danilova, N. V. Kabanova, N. M. Nesterova, N. M. Nikolskaya, S. I. Nikolsky, L. M. Katsarsky, I. N. Kirov, J. N. Stamenov, and V. D. Janminchev, in *International Cosmic Ray Conference* (1977), vol. 8 of *International Cosmic Ray Conference*, p. 129.
- [27] Y. A. Fomin, G. B. Khristiansen, G. B. Kulikov, V. G. Pogorely, V. I. Solovjeva, V. P. Sulakov, and A. V. Trubitsyn, in *International Cosmic Ray Conference* (1991), vol. 2 of *International Cosmic Ray Conference*, p. 85.
- [28] M. Nagano, T. Hara, Y. Hatano, N. Hayashida, S. Kawaguchi, K. Kamata, T. Kifune, and Y. Mizumoto, *J. Phys. G Nucl. Phys.* **10**, 1295 (1984).
- [29] M. A. K. Glasmacher, M. A. Catanese, M. C. Chantell, C. E. Covault, J. W. Cronin, B. E. Fick, L. F. Fortson, J. W. Fowler, K. D. Green, D. B. Kieda, et al., *Astroparticle Physics* **10**, 291 (1999).
- [30] HEGRA-Collaboration, F. Arqueros, J. A. Barrio, K. Bernlöhr, H. Bojahr, I. Calle, J. L. Contreras, J. Cortina, T. Deckers, S. Denninghoff, et al., *Astron. Astrophys.* **359**, 682 (2000), astro-ph/9908202.
- [31] T. Antoni, W. D. Apel, A. F. Badea, K. Bekk, A. Bercuci, J. Blümer, H. Bozdog, I. M. Brancus, A. Chilingarian, et al., *Astroparticle Physics* **24**, 1 (2005), astro-ph/0505413.
- [32] M. Amenomori, X. J. Bi, D. Chen, S. W. Cui, Danzengluobu, L. K. Ding, X. H. Ding, C. Fan, C. F. Feng, Z. Feng, et al., *Astrophys. J.* **678**, 1165 (2008), 0801.1803.
- [33] M. G. Aartsen, R. Abbasi, Y. Abdou, M. Ackermann, J. Adams, J. A. Aguilar, M. Ahlers, D. Altmann, J. Auffenberg, X. Bai, et al., *Phys. Rev. D* **88**, 042004 (2013), 1307.3795.
- [34] R. U. Abbasi, T. Abu-Zayyad, M. Allen, J. F. Amman, G. Archbold, K. Belov, J. W. Belz, S. Y. Ben Zvi, et al., *Phys. Rev. Lett.* **100**, 101101 (2008), astro-ph/0703099.
- [35] J. Abraham, P. Abreu, M. Aglietta, C. Aguirre, D. Allard, I. Allekotte, J. Allen, P. Allison, J. Alvarez-Muñiz, M. Ambrosio, et al., *Phys. Rev. Lett.* **101**, 061101 (2008), 0806.4302.
- [36] T. Abu-Zayyad, R. Aida, M. Allen, R. Anderson, R. Azuma, E. Barcikowski, J. W. Belz, D. R. Bergman, S. A. Blake, R. Cady, et al., *Astrophys. J. Lett.* **768**, L1 (2013), 1205.5067.
- [37] W. D. Apel, J. C. Arteaga-Velázquez, K. Bekk, M. Bertaina, J. Blümer, H. Bozdog, I. M. Brancus, P. Buchholz, E. Cantoni, A. Chiavassa, et al., *Astroparticle Physics* **36**, 183 (2012), 1206.3834.
- [38] N. M. Budnev, A. Chiavassa, O. A. Gress, T. I. Gress, A. N. Dyachok, N. I. Karpov, N. N. Kalmykov, E. E. Korosteleva, V. A. Kozhin, L. A. Kuzmichev, et al., *Astroparticle Physics* **117**, 102406 (2020), 2104.03599.
- [39] S. F. Berezhnev, D. Besson, N. M. Budnev, A. Chiavassa, O. A. Chvalaev, O. A. Gress, A. N. Dyachok, S. N. Epimakhov, A. Haungs, N. I. Karpov, et al., *Nuclear Instruments and Methods in Physics Research A* **692**, 98 (2012), 1201.2122.
- [40] IceCube Collaboration, R. Abbasi, Y. Abdou, M. Ackermann, J. Adams, J. A. Aguilar, M. Ahlers, D. Altmann, K. Andeen, J. Auffenberg, et al., *Astroparticle Physics* **42**, 15 (2013), 1207.3455.
- [41] Z. Cao, F. Aharonian, Axikegu, Y. X. Bai, Y. W. Bao, D. Bastieri, X. J. Bi, Y. J. Bi, W. Bian, A. V. Bukevich, et al., *Phys. Rev. Lett.* **132**, 131002 (2024), 2403.10010.

- [42] T. Abu-Zayyad, K. Belov, D. J. Bird, J. Boyer, Z. Cao, M. Catanese, G. F. Chen, R. W. Clay, C. E. Covault, H. Y. Dai, et al., *Astrophys. J.* **557**, 686 (2001), astro-ph/0010652.
- [43] J. Abraham, P. Abreu, M. Aglietta, E. J. Ahn, D. Allard, I. Allekotte, J. Allen, J. Alvarez-Muñiz, M. Ambrosio, L. Anchordoqui, et al., *Phys. Rev. Lett.* **104**, 091101 (2010), 1002.0699.
- [44] R. U. Abbasi, M. Abe, T. Abu-Zayyad, M. Allen, R. Anderson, R. Azuma, E. Barcikowski, J. W. Belz, D. R. Bergman, S. A. Blake, et al., *Astroparticle Physics* **64**, 49 (2015), 1408.1726.
- [45] K.-H. Kampert and M. Unger, *Astroparticle Physics* **35**, 660 (2012), 1201.0018.
- [46] M. Aguilar, L. Ali Cavasonza, G. Ambrosi, L. Arruda, N. Attig, F. Barao, L. Barrin, A. Bartoloni, S. Başeğmez-du Pree, J. Bates, et al., *Phys. Rept.* **894**, 1 (2021).
- [47] N. A. Schwadron, F. C. Adams, E. R. Christian, P. Desiati, P. Frisch, H. O. Funsten, J. R. Jokipii, D. J. McComas, E. Moe-bius, and G. P. Zank, *Science* **343**, 988 (2014).
- [48] M. Ahlers, *Phys. Rev. Lett.* **117**, 151103 (2016), 1605.06446.
- [49] Pierre Auger Collaboration, A. Aab, P. Abreu, M. Aglietta, I. A. Samarai, I. F. M. Albuquerque, I. Allekotte, A. Almela, J. Alvarez Castillo, J. Alvarez-Muñiz, et al., *Science* **357**, 1266 (2017), 1709.07321.
- [50] A. Aab, P. Abreu, M. Aglietta, I. F. M. Albuquerque, J. M. Al-bury, I. Allekotte, A. Almela, J. Alvarez Castillo, J. Alvarez-Muñiz, G. A. Anastasi, et al., *Astrophys. J.* **891**, 142 (2020), 2002.06172.
- [51] A. W. Strong, I. V. Moskalenko, and V. S. Ptuskin, *Annual Review of Nuclear and Particle Science* **57**, 285 (2007), astro-ph/0701517.
- [52] R. Trotta, G. Jóhannesson, I. V. Moskalenko, T. A. Porter, R. Ruiz de Austri, and A. W. Strong, *Astrophys. J.* **729**, 106 (2011), 1011.0037.
- [53] M. J. Boschini, S. Della Torre, M. Gervasi, D. Grandi, G. Jóhannesson, G. La Vacca, N. Masi, I. V. Moskalenko, S. Pensotti, T. A. Porter, et al., *Astrophys. J. Supp.* **250**, 27 (2020), 2006.01337.
- [54] X. Pan and Q. Yuan, *Research in Astronomy and Astrophysics* **23**, 115002 (2023), 2403.06719.
- [55] A. U. Abeysekara, A. Albert, R. Alfaro, C. Alvarez, J. D. Álvarez, R. Arceo, J. C. Arteaga-Velázquez, D. Avila Rojas, H. A. Ayala Solares, A. S. Barber, et al., *Science* **358**, 911 (2017), 1711.06223.
- [56] F. Aharonian, Q. An, L. X. Axikegu, Bai, Y. X. Bai, Y. W. Bao, D. Bastieri, X. J. Bi, Y. J. Bi, H. Cai, J. T. Cai, et al., *Phys. Rev. Lett.* **126**, 241103 (2021), 2106.09396.
- [57] Q. Yuan, S.-J. Lin, K. Fang, and X.-J. Bi, *Phys. Rev. D* **95**, 083007 (2017), 1701.06149.
- [58] N. Tomassetti and F. Donato, *Astron. Astrophys.* **544**, A16 (2012), 1203.6094.
- [59] Y.-Q. Guo, Z. Tian, and C. Jin, *Astrophys. J.* **819**, 54 (2016), 1509.08227.
- [60] Y.-Q. Guo and Q. Yuan, *Phys. Rev. D* **97**, 063008 (2018), 1801.05904.
- [61] E. S. Seo and V. S. Ptuskin, *Astrophys. J.* **431**, 705 (1994).
- [62] C. Evoli, D. Gaggero, A. Vittino, G. Di Bernardo, M. Di Mauro, A. Ligorini, P. Ullio, and D. Grasso, *J. Cosmol. Astropart. Phys.* **2017**, 015 (2017), 1607.07886.
- [63] L. J. Gleeson and W. I. Axford, *Astrophys. J.* **154**, 1011 (1968).
- [64] Q. Luo, B.-Q. Qiao, W. Liu, S.-W. Cui, and Y.-Q. Guo, *Astrophys. J.* **930**, 82 (2022), 2110.00501.
- [65] P.-P. Zhang, B.-Q. Qiao, Q. Yuan, S.-W. Cui, and Y.-Q. Guo, *Phys. Rev. D* **105**, 023002 (2022), 2107.08280.
- [66] R. N. Manchester, G. B. Hobbs, A. Teoh, and M. Hobbs, *Astron. J.* **129**, 1993 (2005), astro-ph/0412641.
- [67] V. Berezhinsky, A. Gazizov, and S. Grigorieva, *Phys. Rev. D* **74**, 043005 (2006), hep-ph/0204357.
- [68] A. Yushkov, in *36th International Cosmic Ray Conference (ICRC2019)* (2019), vol. 36 of *International Cosmic Ray Conference*, p. 482.
- [69] R. Aloisio, V. Berezhinsky, and A. Gazizov, *Astroparticle Physics* **34**, 620 (2011), 0907.5194.
- [70] R. Aloisio, V. Berezhinsky, and A. Gazizov, *Astroparticle Physics* **39**, 129 (2012), 1211.0494.
- [71] A. M. Hillas, *Journal of Physics G Nuclear Physics* **31**, 95 (2005).
- [72] S. Mollerach and E. Roulet, *J. Cosmol. Astropart. Phys.* **2019**, 017 (2019), 1812.04026.
- [73] M. Aguilar, L. A. Cavasonza, B. Alpat, G. Ambrosi, L. Arruda, N. Attig, F. Barao, L. Barrin, A. Bartoloni, S. Başeğmez-du Pree, et al., *Phys. Rev. Lett.* **127**, 021101 (2021).
- [74] M. Aguilar, L. A. Cavasonza, M. S. Allen, B. Alpat, G. Ambrosi, L. Arruda, N. Attig, F. Barao, L. Barrin, A. Bartoloni, et al., *Phys. Rev. Lett.* **126**, 041104 (2021).
- [75] M. Aguilar, L. Ali Cavasonza, G. Ambrosi, L. Arruda, N. Attig, F. Barao, L. Barrin, A. Bartoloni, S. Başeğmez-du Pree, R. Battiston, et al., *Phys. Rev. Lett.* **124**, 211102 (2020).
- [76] M. Aguilar, L. Ali Cavasonza, B. Alpat, G. Ambrosi, L. Arruda, N. Attig, S. Aupetit, P. Azzarello, A. Bachlechner, F. Barao, et al., *Phys. Rev. Lett.* **121**, 051103 (2018).
- [77] M. Aguilar, L. Ali Cavasonza, B. Alpat, G. Ambrosi, L. Arruda, N. Attig, S. Aupetit, P. Azzarello, A. Bachlechner, F. Barao, et al., *Phys. Rev. Lett.* **119**, 251101 (2017).
- [78] H. S. Ahn, P. Allison, M. G. Bagliesi, L. Barbier, J. J. Beatty, G. Bigongiari, T. J. Brandt, J. T. Childers, N. B. Conklin, S. Coutu, et al., *Astrophys. J.* **707**, 593 (2009), 0911.1889.
- [79] J. R. Hörandel, *Astroparticle Physics* **19**, 193 (2003), astro-ph/0210453.
- [80] M. G. Aartsen, M. Ackermann, J. Adams, J. A. Aguilar, M. Ahlers, M. Ahrens, C. Alispach, K. Andeen, T. Anderson, I. Ansseau, et al., *Phys. Rev. D* **100**, 082002 (2019), 1906.04317.
- [81] M. G. Aartsen, R. Abbasi, M. Ackermann, J. Adams, J. A. Aguilar, M. Ahlers, M. Ahrens, C. Alispach, N. M. Amin, K. Andeen, et al., *Phys. Rev. D* **102**, 122001 (2020), 2006.05215.
- [82] A. Aab, P. Abreu, M. Aglietta, J. M. Albury, I. Allekotte, A. Almela, J. Alvarez Castillo, J. Alvarez-Muñiz, R. Alves Batista, G. A. Anastasi, et al., *Phys. Rev. Lett.* **125**, 121106 (2020), 2008.06488.
- [83] A. Aab, P. Abreu, M. Aglietta, J. M. Albury, I. Allekotte, A. Almela, J. Alvarez Castillo, J. Alvarez-Muñiz, R. Alves Batista, G. A. Anastasi, et al., *Phys. Rev. D* **102**, 062005 (2020), 2008.06486.
- [84] R. U. Abbasi, M. Abe, T. Abu-Zayyad, M. Allen, R. Azuma, E. Barcikowski, J. W. Belz, D. R. Bergman, S. A. Blake, R. Cady, et al., *Astroparticle Physics* **80**, 131 (2016).
- [85] R. U. Abbasi, M. Abe, T. Abu-Zayyad, M. Allen, R. Azuma, E. Barcikowski, J. W. Belz, D. R. Bergman, S. A. Blake, R. Cady, et al., *Astrophys. J.* **865**, 74 (2018), 1803.01288.
- [86] A. Turundaevskiy, D. Karmanov, I. Kovalev, I. Kudryashov, A. Kurganov, A. Panov, and D. Podorozhny, *Advances in Space Research* **70**, 2696 (2022).
- [87] A. D. Panov, J. H. Adams, H. S. Ahn, G. L. Bashinzhagyan, J. W. Watts, J. P. Wefel, J. Wu, O. Ganel, T. G. Guzik, V. I. Zatsepin, et al., *Bulletin of the Russian Academy of Sciences, Physics* **73**, 564 (2009), 1101.3246.

- [88] W. D. Apel, J. C. Arteaga-Velázquez, K. Bekk, M. Bertaina, J. Blümer, H. Bozdog, I. M. Brancus, E. Cantoni, A. Chiavassa, F. Cossavella, et al., *Astroparticle Physics* **47**, 54 (2013).
- [89] R. Abbasi, Y. Abdou, M. Ackermann, J. Adams, J. A. Aguilar, M. Ahlers, D. Altmann, K. Andeen, J. Auffenberg, X. Bai, et al., *Nuclear Instruments and Methods in Physics Research A* **700**, 188 (2013), 1207.6326.
- [90] Pierre Auger Collaboration, *J. Cosmol. Astropart. Phys.* **2013**, 026 (2013), 1301.6637.
- [91] R. U. Abbasi, M. Abe, T. Abu-Zayyad, M. Allen, Y. Arai, E. Barcikowski, J. W. Belz, D. R. Bergman, S. A. Blake, R. Cady, et al., *Astrophys. J.* **909**, 178 (2021), 1012.10372.
- [92] S. Sakakibara, H. Ueno, K. Fujimoto, I. Kondo, and K. Nagashima, in *International Cosmic Ray Conference* (1973), vol. 2 of *International Cosmic Ray Conference*, p. 1058.
- [93] T. Gombosi, J. Kóta, A. J. Somogyi, A. Varga, B. Betev, L. Katsarski, S. Kavlaikov, and I. Khiriv, in *International Cosmic Ray Conference* (1975), vol. 2 of *International Cosmic Ray Conference*, pp. 586–591.
- [94] M. Bercovitch and S. P. Agrawal, in *International Cosmic Ray Conference* (1981), vol. 10 of *International Cosmic Ray Conference*, pp. 246–249.
- [95] V. V. Alexeyenko, A. E. Chudakov, E. N. Gulieva, and V. G. Sbarschikov, in *International Cosmic Ray Conference* (1981), vol. 2 of *International Cosmic Ray Conference*, p. 146.
- [96] T. Thambyahpillai, in *International Cosmic Ray Conference* (1983), vol. 3 of *International Cosmic Ray Conference*, p. 383.
- [97] K. Nagashima, S. Sakakibara, A. G. Fenton, and J. E. Humble, *Planet. Space Sci.* **33**, 395 (1985).
- [98] D. B. Swinson and K. Nagashima, *Planet. Space Sci.* **33**, 1069 (1985).
- [99] Y. M. Andreyev, A. E. Chudakov, V. A. Kozyarivsky, A. M. Sidorenko, T. I. Tulupova, and A. V. Voevodsky, in *International Cosmic Ray Conference* (1987), vol. 2 of *International Cosmic Ray Conference*, p. 22.
- [100] K. Nagashima, K. Fujimoto, S. Sakakibara, Z. Fujii, H. Ueno, K. Murakami, and I. Morishita, *Nuovo Cimento C Geophysics Space Physics C* **12**, 695 (1989).
- [101] K. Munakata, S. Yasue, S. Mori, C. Kato, M. Koyama, S. Akahane, Z. Fujii, H. Ueno, J. E. Humble, A. G. Fenton, et al., in *International Cosmic Ray Conference* (1995), vol. 4 of *International Cosmic Ray Conference*, p. 639.
- [102] S. Mori, S. Yasue, K. Munakata, C. Kato, S. Akahane, M. Koyama, and T. Kitawada, in *International Cosmic Ray Conference* (1995), vol. 4 of *International Cosmic Ray Conference*, p. 648.
- [103] K. B. Fenton, A. G. Fenton, and J. E. Humble, in *International Cosmic Ray Conference* (1995), vol. 4 of *International Cosmic Ray Conference*, p. 635.
- [104] M. Aglietta, B. Alessandro, P. Antonioli, F. Arneodo, L. Bergamasco, M. Bertaina, A. Bosio, A. Castellina, C. Castagnoli, A. Chiavassa, et al., in *International Cosmic Ray Conference* (1995), vol. 2 of *International Cosmic Ray Conference*, p. 800.
- [105] M. Aglietta, B. Alessandro, P. Antonioli, F. Arneodo, L. Bergamasco, M. Bertaina, A. Bosio, A. Castellina, C. Castagnoli, A. Chiavassa, et al., *Astrophys. J.* **470**, 501 (1996).
- [106] K. Munakata, T. Kiuchi, S. Yasue, C. Kato, S. Mori, K. S. Hirata, K. Kihara, Y. Oyama, M. Mori, K. Fujita, et al., *Phys. Rev. D* **56**, 23 (1997).
- [107] M. Ambrosio, R. Antolini, A. Baldini, G. C. Barbarino, B. C. Barish, G. Battistoni, Y. Becherini, R. Bellotti, C. Bemporad, P. Bernardini, et al., *Phys. Rev. D* **67**, 042002 (2003), astro-ph/0211119.
- [108] M. Amenomori, S. Ayabe, S. W. Cui, Danzengluobu, L. K. Ding, X. H. Ding, C. F. Feng, Z. Y. Feng, X. Y. Gao, Q. X. Geng, et al., *Astrophys. J. Lett.* **626**, L29 (2005), astro-ph/0505114.
- [109] G. Guillian, J. Hosaka, K. Ishihara, J. Kameda, Y. Koshio, A. Minamino, C. Mitsuda, M. Miura, S. Moriyama, M. Nakahata, et al., *Phys. Rev. D* **75**, 062003 (2007), astro-ph/0508468.
- [110] M. Aglietta, V. V. Alekseenko, B. Alessandro, P. Antonioli, F. Arneodo, L. Bergamasco, M. Bertaina, R. Bonino, A. Castellina, A. Chiavassa, et al., *Astrophys. J. Lett.* **692**, L130 (2009), 0901.2740.
- [111] V. V. Alekseenko, A. B. Cherniaev, D. D. Djappuev, A. U. Kudjaev, O. I. Michailova, Y. V. Stenkin, V. I. Stepanov, and V. I. Volchenko, *Nuclear Physics B Proceedings Supplements* **196**, 179 (2009), 0902.2967.
- [112] A. A. Abdo, B. T. Allen, T. Aune, D. Berley, S. Casanova, C. Chen, B. L. Dingus, R. W. Ellsworth, L. Fleyscher, R. Fleyscher, et al., *Astrophys. J.* **698**, 2121 (2009), 0806.2293.
- [113] R. Abbasi, Y. Abdou, T. Abu-Zayyad, J. Adams, J. A. Aguilar, M. Ahlers, K. Andeen, J. Auffenberg, X. Bai, M. Baker, et al., *Astrophys. J.* **718**, L194 (2010), 1005.2960.
- [114] R. Abbasi, Y. Abdou, T. Abu-Zayyad, M. Ackermann, J. Adams, J. A. Aguilar, M. Ahlers, M. M. Allen, D. Altmann, K. Andeen, et al., *Astrophys. J.* **746**, 33 (2012), 1109.1017.
- [115] M. G. Aartsen, R. Abbasi, Y. Abdou, M. Ackermann, J. Adams, J. A. Aguilar, M. Ahlers, D. Altmann, K. Andeen, J. Auffenberg, et al., *Astrophys. J.* **765**, 55 (2013), 1210.5278.
- [116] B. Bartoli, P. Bernardini, X. J. Bi, Z. Cao, S. Catalanotti, S. Z. Chen, T. L. Chen, S. W. Cui, B. Z. Dai, A. D’Amone, et al., *Astrophys. J.* **809**, 90 (2015).
- [117] M. Amenomori, X. J. Bi, D. Chen, T. L. Chen, W. Y. Chen, S. W. Cui, Danzengluobu, L. K. Ding, C. F. Feng, Z. Feng, et al., *Astrophys. J.* **836**, 153 (2017), 1701.07144.
- [118] B. Bartoli, P. Bernardini, X. J. Bi, Z. Cao, S. Catalanotti, S. Z. Chen, T. L. Chen, S. W. Cui, B. Z. Dai, A. D’Amone, et al., *Astrophys. J.* **861**, 93 (2018), 1805.08980.
- [119] M. Ajello, L. Baldini, G. Barbiellini, D. Bastieri, K. Bechtol, R. Bellazzini, E. Bissaldi, R. D. Blandford, R. Bonino, E. Bottacini, et al., *Astrophys. J.* **883**, 33 (2019).
- [120] The Pierre Auger Collaboration, A. A. Halim, P. Abreu, M. Aglietta, I. Allekotte, K. Almeida Cheminant, A. Almela, R. Aloisio, J. Alvarez-Muñiz, A. Ambrosone, et al., *arXiv e-prints arXiv:2408.05292* (2024), 2408.05292.
- [121] O. Adriani, Y. Akaike, K. Asano, Y. Asaoka, E. Berti, G. Bigongiari, W. R. Binns, M. Bongi, P. Brogi, A. Bruno, et al., *Phys. Rev. Lett.* **126**, 241101 (2021), 2106.08036.
- [122] S. N. Zhang, O. Adriani, S. Albergo, G. Ambrosi, Q. An, T. W. Bao, R. Battiston, X. J. Bi, Z. Cao, J. Y. Chai, et al., in *Proc. SPIE* (2014), vol. 9144, p. 91440X, 1407.4866.
- [123] X. Pan, W. Jiang, C. Yue, S.-J. Lei, Y.-X. Cui, and Q. Yuan, *Nuclear Science and Techniques* **35**, 149 (2024), 2407.16973.